The Alzheimer's Aβ-peptide is deposited at sites of complement activation in pathologic deposits associated with aging and age-related macular degeneration

Lincoln V. Johnson*, William P. Leitner, Alexander J. Rivest, Michelle K. Staples, Monte J. Radeke, and Don H. Anderson

Center for the Study of Macular Degeneration, Neuroscience Research Institute, University of California, Santa Barbara, CA 93016

Edited by Jeremy Nathans, Johns Hopkins University School of Medicine, Baltimore, MD, and approved July 11, 2002 (received for review April 5, 2002)

Age-related macular degeneration (AMD) is a leading cause of irreversible vision loss in older individuals worldwide. The disease is characterized by abnormal extracellular deposits, known as drusen, that accumulate along the basal surface of the retinal pigmented epithelium. Although drusen deposition is common in older individuals, large numbers of drusen and/or extensive areas of confluent drusen represent a significant risk factor for AMD. Widespread drusen deposition is associated with retinal pigmented epithelial cell dysfunction and degeneration of the photoreceptor cells of the neural retina. Recent studies have shown that drusen contain a variety of immunomodulatory molecules, suggesting that the process of drusen formation involves local inflammatory events, including activation of the complement cascade. Similar observations in Alzheimer's disease (AD) have lead to the hypothesis that chronic localized inflammation is an important element of AD pathogenesis, with significant neurodegenerative consequences. Accordingly, the amyloid beta (Aβ) peptide, a major constituent of neuritic plaques in AD, has been implicated as a primary activator of complement in AD. Here we show that Aβ is associated with a substructural vesicular component within drusen. Aβ colocalizes with activated complement components in these ''amyloid vesicles,'' thereby identifying them as potential primary sites of complement activation. Thus, Aβ deposition could be an important component of the local inflammatory events that contribute to atrophy of the retinal pigmented epithelium, drusen biogenesis, and the pathogenesis of AMD.

Current theories of Alzheimer's disease (AD) pathogenesis include inflammatory processes as significant contributors to the disease process (1). Chronic local inflammation, including both direct and bystander cell damage attributable to complement-mediated attack, exacerbates the effects of primary AD pathogenic stimuli. Amyloid beta (Aβ) has been implicated in activation of the complement cascade (2) and is a major component of AD plaques, where it colocalizes with activated complement components, the C5b-9 membrane attack complex (MAC), acute phase reactants, and other inflammatory mediators (3–5).

New evidence suggests that a strikingly similar, chronic local inflammatory component is also associated with the formation of drusen, the age-related extracellular deposits that are often linked with age-related macular degeneration (AMD) (6–9). AMD is a retinal degenerative disease that leads to loss of central vision, and affects 5–10% of the population over 60 years of age. Drusen form between the basal surface of an epithelial monolayer derived from neuroectoderm that is known as the retinal pigmented epithelium (RPE), and a basement membrane complex called Bruch's membrane (Fig. 1). Small numbers of drusen are present in the eyes of many older individuals; however, numerous and/or confluent drusen are associated clinically with geographic atrophy of the RPE (10) and with a significantly increased risk of developing the exudative (or neovascular) form of AMD (11). In the absence of a viable RPE, degeneration of adjacent photoreceptor cells and the loss of vision characteristic of AMD ensue.

Interestingly, many of the proteins present in drusen are also components of the plaques and deposits that characterize diseases such as atherosclerosis, skin elastosis, glomerulonephritis, and AD (12). A number of these are known immunomodulators, inflammatory mediators, and/or acute phase reactants (6, 7, 9), immunoglobulin molecules and activated components of the complement system are associated with drusen, and with RPE cells that flank or overlie drusen (7). These findings implicate local inflammatory events in drusen formation, and strongly suggest that complement-mediated attack on the RPE aggravates the effects of the pathogenic stimuli that give rise to AMD (6, 8, 9). We have proposed that the debris derived from compromised RPE cells, which becomes entrapped between the RPE monolayer and Bruch's membrane, may serve as a chronic inflammatory stimulus and a nucleation site for drusen formation (6, 7).

In this investigation, we identify the Alzheimer's Aβ protein as a potential activator of the complement cascade in the context of drusen formation. We show that Aβ colocalizes with activation-specific fragments of complement C3 in unique substructural domains within drusen, and we present evidence indicating that these Aβ-rich elements are the likely by-products of degenerate RPE cells. These results suggest that Aβ deposition may be a key contributor to RPE atrophy, drusen biogenesis, and the pathogenesis of AMD.

Methods

Tissues and Cells. Human donor eyes were provided by the Lions Eye Bank of Oregon (Portland) and the Doheny Eye and Tissue Transplant Bank (Goleta, CA). Specimens from ten donors (ages 49–89 years) with postmortem times to fixation from 4.5 to 6 h were examined. Three were from donors with clinically documented atrophic AMD. Samples of both macular and surrounding RPE/choroid that contain drusen were identified and excised under a dissecting microscope. RPE cell cultures were derived from third-trimester human eyes (Advanced Bioscience Resources, Alameda, CA) as described (13). An SV40 transformed human RPE cell line (SV40 RPE) (14) and primary neonatal human diploid fibroblast cultures (Clonetics, San Diego) were also analyzed.

Confocal Immunofluorescence Microscopy. Vibratome sections of agarose-embedded tissue specimens, and cells grown on glass coverslips, were processed for laser scanning confocal immuno-

This paper was submitted directly (Track II) to the PNAS office.

Abbreviations: AD, Alzheimer's disease; AMD, age-related macular degeneration; Aβ, amyloid beta; APP, amyloid precursor protein; RPE, retinal pigmented epithelium.

*To whom reprint requests should be addressed. E-mail: l.johnso@lifesci.ucsb.edu.

 www.pnas.org/cgi/doi/10.1073/pnas.192203399

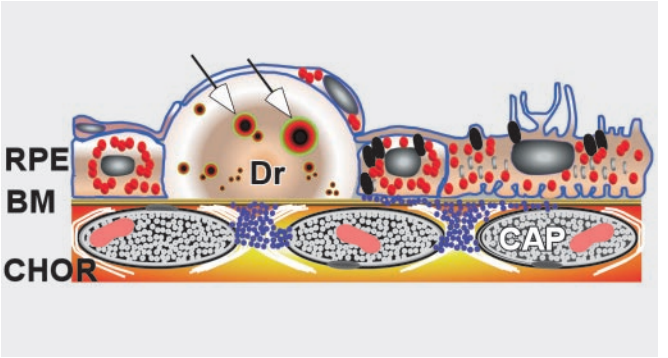

Fig. 1. Diagram depicting the anatomical relationships among the retinal pigmented epithelium (RPE), Bruch's membrane (BM), and drusen (Dr). Vesicles containing amyloid β that likely represent primary sites of complement activation are identified within drusen (arrows). CHOR, choroidal vasculature; CAP, capilllary.

fluorescence microscopy (15). Sections were blocked with normal donkey serum in 100 mM sodium phosphate buffer (pH 7.1) containing 0.5% BSA, 0.05% Triton X-100, and 0.1% sodium azide and then exposed to primary antibodies diluted in the same buffer. Amyloid precursor protein (APP) and Aβ antibodies with documented binding activity in AD plaques (16–18) were used: (*i*) mouse anti-Aβ clone 6E10 (18), a monoclonal antibody specific for an epitope within amino acids 1–16 of the Aβ peptide (Chemicon); (*ii*) mouse anti-Aβ clone 4G8 (17), a monoclonal antibody specific for an epitope within amino acids 17–24 of the Aβ peptide (Signet Laboratories, Dedham, MA); (*iii*) mouse anti-Aβ precursor protein (APP) clone 22C11 (16), a monoclonal antibody specific for an epitope outside the Aβ peptide within N-terminal amino acids 66–81 of human APP (Chemicon); and (*iv*) goat anti-APP, a polyclonal antibody generated against an APP-specific peptide consisting of N-terminal amino acids 44–63 (Chemicon). A monoclonal antibody specific for a neo-epitope on complement iC3b (Quidel, San Diego) was used to identify complement activation sites (6). Primary antibody incubation was followed by rinsing and overnight incubation in species-specific donkey secondary antibodies conjugated with indocarbocyanine-2, -3, or -5 (Jackson ImmunoResearch). Control studies that included omission of primary antibody, or substitution with a similar concentration of irrelevant antibody, confirmed the absence of nonspecific labeling by secondary antibodies. Specificity of the 4G8 antibody was confirmed by adsorption with a twofold molar excess of $A\beta_{1\rightarrow42}$ peptide (BioSource International, Camarillo, CA). Sections were mounted in glycerol containing *N*-propyl-gallate as an antiquenching agent and examined using a Bio-Rad 1024 laser scanning confocal microscope. Images were acquired with LASERSHARP software (Bio-Rad); pseudo double-labeled images were generated by optimizing the Cy3 (red) channel to allow visualization of autofluorescence from lipofuscin pigment in RPE cells and Bruch's membrane.

PCR. Endpoint PCR was used to assess APP isoform expression using primers that flank the alternative splice site of APP and generate PCR amplicons of 87, 144, 255, and 312 bp, reflecting the expression of the APP_{695}, APP_{714}, APP_{751}, and APP_{770} isoforms, respectively (19). Total RNA was extracted from first- or second-passage primary RPE cultures, SV40 RPE cells, and from fourth-passage fibroblasts using RNeasy Mini kits (Qiagen, Valencia, CA). Total RNA from whole normal adult human brain (Lot 7080717) and fetal human brain (Lot 6120259) was obtained from CLONTECH. Following DNase treatment, cDNAs were synthesized from RNAs by using Superscript II reverse transcriptase (Invitrogen) primed with random hexamers. PCR reactions contained 400 nM forward and reverse primers, 1× PCR buffer (Promega), 2.5 mM $MgCl_2$, 200 mM dNTPs, *Taq* Platinum DNA polymerase (Invitrogen), and 28 ng cDNA. DNA was melted at 95°C for 2 min and the PCR reaction was run through 40 cycles at 95°C for 15 s and 60°C for 1 min. The reaction products were separated on 1.8% agarose gels containing ethidium bromide.

Real-time quantitative PCR (QPCR) analyses (20) of the relative expression levels of APP_{751}, APP_{695}, and β-secretase were performed using Prism 7700 sequence detection instrumentation (PE Applied Biosystems). QPCR reactions used the cDNA sources described above as templates and specific primers for human APP_{751} (21), APP_{695}, and β-secretase (300 nM each). Primers for 18s ribosomal RNA (18s rRNA) were used to provide normalizing parameters (22). APP_{695} primers were designed to cross the internal splice site between exons six and nine (GenBank accession no. D87675). β-secretase primers were based on published sequence information (GenBank accession no. NM012104). Primer sequences: APP_{751} (forward, 5′-GATGACGTCTTGGCCAACA-3′; reverse, 5′-CTTTGTTTGAACCCACATCTTC-3′), APP_{695} (forward, 5′-TGGAAGAGGTGGTTCGAGTTCCTA-3′; reverse, 5′-CCTCAAGCCTCTCTTTGGCTTT-3′), β-secretase (forward, 5′-CAGTCATCCACGGGCACTG-3′; reverse, 5′-CTGAACTCATCGTGCACATGG-3′), 18s rRNA (forward, 5′-CGGCTACCACATCCAAGGAA-3′; reverse, 5′-GCTGGAATTACCGCGGCT-3′). Triplicate amplification reactions were performed for each sample (22) in a minimum of seven separate assays. SYBR Green I (Molecular Probes) was used as a quantitative fluorescent marker of amplicon production (23). Data were analyzed using the delta, delta C_t method (PE Applied Biosystems User Bulletin 2); normalized values were expressed as a ratio relative to the adult brain sample that was arbitrary set at 1.0. Samples of the amplification products were analyzed on 1.8% agarose gels containing ethidium bromide to confirm the presence of amplicons of the predicted sizes (125 bp for APP_{695}; 378 bp for APP_{751}; 121 bp for β-secretase; 67 bp for 18s rRNA).

Results

Immunohistochemistry. Laser scanning confocal immunofluorescence microscopy revealed numerous elements within hard drusen that are prominently stained by anti-Aβ antibodies (Fig. 2). These spherical structures range from 2 to 10 μm in diameter and are readily detected in both macular and peripheral drusen from donors with and without clinical AMD. Some drusen are densely packed with "amyloid vesicles," accounting for a significant proportion of their total volume (Fig. 2*A*). Some smaller drusen may contain only a single large vesicle that occupies a substantial portion of the drusen mass (Fig. 2*B*). In some instances, vesicles appear to be in the process of budding or fusing (Fig. 2 *A*, *C*, and *D*). By projecting a series of serial optical sections, the three-dimensional configuration of amyloid vesicles is apparent (Fig. 2*D*). Aβ immunoreactivity is associated most strongly and consistently with the outer shells or rims of the vesicles (Fig. 2 *B* and *C*). However, in many there is discernible interior substructure in the form of flocculent material and/or concentric ring-like elements, which may also show immunoreactivity (Fig. 2 *A* and *B*).

Punctate Aβ immunoreactivity is identified in the cytoplasm of RPE cells *in situ*, especially in those cells that overlie drusen (Fig. 2 *E* and *F*), as well as in the cytoplasm of cultured RPE cells (Fig. 2*K*). This labeling pattern is consistent with the reported distribution of Aβ in vesicular elements of the endosomal–lysosomal system, Golgi apparatus, and endoplasmic reticulum (24). Some RPE cells that are displaced by or flank drusen contain Aβ immunoreactive structures that are similar in appearance to the amyloid vesicles in drusen (Fig. 2*E*). Secondary

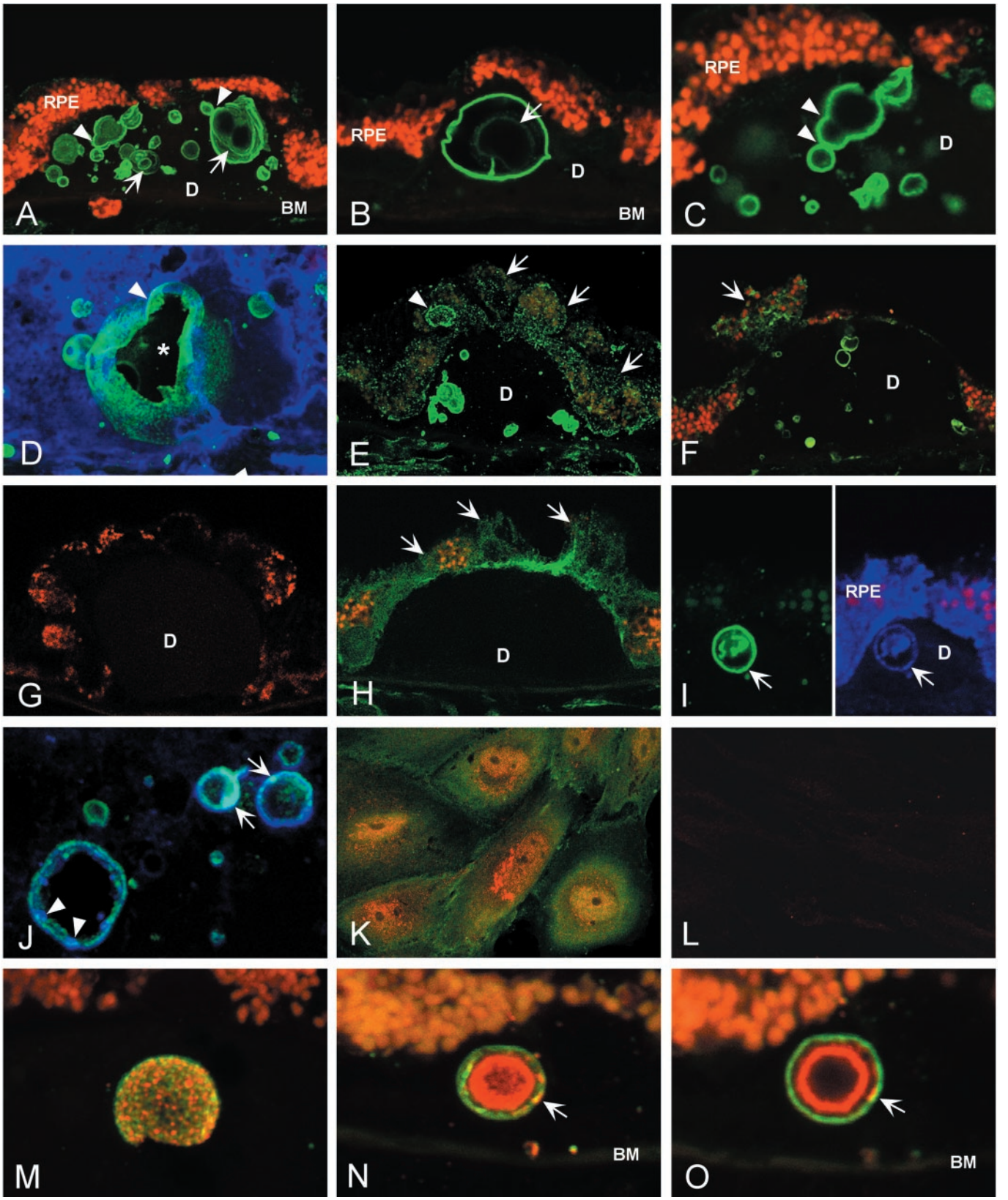

Fig. 2. Immunolocalization of APP and Aβ in drusen by laser scanning confocal immunofluorescence microscopy. (*A–C*) Anti-Aβ (6E10) binds vesicular elements within drusen (green; Cy 2 channel) of an 84-year-old male with clinical diagnosis of atrophic AMD. These ''amyloid vesicles'' frequently exhibit a multilamellar structure (arrows in *A* and *B*). Aβ immunoreactivity is concentrated on the outer shell of the vesicle; varying levels of Aβ are associated with the inner lamellae. Images suggesting the fusion and/or budding of vesicles are often observed (arrowheads in *A* and *C*). Autofluorescent lipofuscin particles are concentrated in the RPE cytoplasm (red; Cy3 channel). (*D*) A serial reconstruction of 34 0.3-μm optical sections showing a large amyloid vesicle and several smaller vesicles labeled with anti-Aβ (6E10); sectioning has partially exposed the central cavity (asterisk). Evidence of fusion or budding is apparent near the top of the vesicle (arrowhead)

antibody controls (Fig. 2*G*) show no evidence of nonspecific binding. Adsorption of anti-Aβ antibodies with A$\beta_{1\rightarrow42}$ peptide significantly reduces immunolabeling (Fig. 2*L*).

To distinguish Aβ immunoreactivity from that of APP, the immunoreactivity patterns of three monoclonal antibodies were compared. Both the 6E10 and 4G8 anti-Aβ antibodies label amyloid vesicles within drusen (Fig. 2 *A–F*). In contrast, the 22C11 antibody, which binds a non-Aβ epitope in the N-terminal portion of APP, shows particulate staining of RPE cytoplasm (Fig. 2*H*), but does not label the amyloid vesicles (Fig. 2*H*). Some 6E10-positive vesicles (Fig. 2*I Left*) also exhibit less intense anti-APP labeling when using an APP polyclonal antibody (Fig. 2*I Right*). Discrete as well as overlapping zones of punctate APP and Aβ labeling are sometimes apparent in the outer vesicular shells (Fig. 2*J*). These observations indicate that the Aβ peptide, rather than APP, is the predominant constituent.

Recently, we reported that substructural elements within drusen that are identical in size and shape to the amyloid vesicles described above contain activation-specific fragments of complement C3 (6). Double immunolabeling experiments confirm that most of these vesicles display both iC3b and Aβ immunoreactivities, but their respective distributions differ. Single optical sections show that Aβ is concentrated in the outer shell where punctate regions of anti-iC3b labeling are also apparent (Fig. 2 *M–O*). In serial reconstructions of 0.3-μm optical sections, the respective distributions of iC3b and Aβ on the outer shell of a large amyloid vesicle appear random (Fig. 2*M*). In cross-sections through the vesicular core, however, iC3b immunoreactivity predominates. The co-distribution of iC3b and Aβ in the vesicles is shown most dramatically in Fig. 2*N* (projection series) and Fig. 2*O* (single optical section), where an Aβ-rich outer shell envelops a concentric inner sphere that contains iC3b.

PCR. Endpoint PCR analysis detects transcripts for all three major APP isoforms in RPE and fibroblast cultures (Fig. 3*A*). In both, APP_{770} and APP_{751} appear to be more abundant than APP_{695}. As expected (25), APP_{695} is most abundant in both adult and fetal brain. The rare APP_{714} isoform was not detected; however, an unidentified $\approx$450-bp amplicon was present in all samples except fetal brain.

In quantitative PCR (QPCR) assays (Fig. 3 *B* and *C*, Table 1), RPE cultures show expression levels for APP_{751} that are not significantly different from those in adult or fetal brain, or in fibroblasts. As anticipated, APP_{695} levels are significantly higher in the brain samples than in RPE cells or fibroblasts. Primary and SV40 RPE cells have APP_{695} transcript levels that are 20- and 11-fold lower, respectively, than those in adult brain. The APP_{695} transcript level in fibroblasts is equivalent to those of the RPE samples. QPCR analyses also demonstrate that RPE cells and fibroblasts contain β-secretase transcripts that are 25–50% the levels in either adult or fetal brain.

Discussion

Recent studies have shown that age-related ocular drusen contain a substantial number of proteins that are also components of AD plaques, as well as the extracellular deposits associated with other age-related disorders (6, 7, 9, 12, 26, 27). Because many of these shared molecular constituents are proteins functionally linked to the process of inflammation or its aftermath, we have hypothesized that drusen are a by-product of chronic, localized inflammatory processes and endogenous anti-inflammatory responses that may play an important role in the pathogenesis of AMD (6–9).

Inflammatory proteins identified in drusen include terminal complement components and the membrane attack complex (MAC), inhibitors of complement activation (6, 26), and several potential complement-activating molecules (12, 28). During the process of complement activation, specific proteolytic fragments of complement C3 become covalently attached at primary sites of activation (reviewed in ref. 29). Antibodies to activation-specific C3 fragments label vesicular substructural elements within drusen, thereby designating them as potential sites of complement activation (6). Here, we show that the Alzheimer's Aβ peptide is associated with these same vesicular elements (Fig. 2 *M–O*; ref. 6), thus suggesting that Aβ may play a primary role in the activation of complement-mediated events during drusen formation. The colocalization of Aβ and iC3b immunoreactivity in the outer vesicular shell (Fig. 2 *M* and *N*) is consistent with this interpretation; however, the significance of the iC3b-rich inner sphere has not been established.

Previous studies have documented Aβ as a primary activator of the complement cascade in AD (1). Aβ is a major component of neuritic plaques where it colocalizes with activated complement components and the MAC (3, 30). Activation of both the classical and alternative complement pathways can be induced by Aβ (2, 3). Although several known drusen constituents including serum amyloid P (31), clusterin (32), apolipoprotein E (33), α_1-antichymotrypsin (34), and transthyretin (35) can form complexes with and modulate the molecular properties of Aβ, the existing evidence for Aβ as a molecular constituent of drusen is conflicting (12, 36).

Small vesicular structures have been identified in previous ultrastructural studies of drusen (11, 37–40). Most notably, Ulshafer *et al.* (41) identified two types of substructural elements: irregular globular masses and spherical entities with electron dense cores surrounded by concentric layers of ''crystalline spicules.'' The latter structures appear to be highly similar, if not identical, to the amyloid vesicles identified in this study. Also of potential significance is a report showing that Aβ peptides can self-assemble into spherical macromolecular ag-

and on the far interior wall. (*E* and *F*) Anti-Aβ labeling of RPE cells (*E*, 6E10; *F*, 4G8). Fine, granular Aβ immunoreactivity is observed in the cytoplasm of RPE cells overlying drusen (arrows). One RPE cell contains an Aβ-positive structure that is similar in size and shape to the amyloid vesicles within drusen (arrowhead in *E*). (*G*) Secondary antibody control illustrating the absence of binding to drusen or RPE cells by the Cy2-conjugated donkey anti-mouse Ig used for the detection of anti-Aβ and anti-APP monoclonal antibodies. Autofluorescent lipofuscin particles (red; Cy3 channel) mark the RPE cells. (*H*) Anti-APP (22C11) localizes APP to the RPE cell cytoplasm (arrows); however, drusen are not labeled. (*I* and *J*) Double-label images illustrating labeling patterns for APP (blue; Cy5 channel) and Aβ (green; Cy2 channel). (*I Left*) Anti-Aβ (6E10) strongly labels a single large amyloid vesicle (arrow); (*Right*) In the same section, anti-APP (N-terminal peptide 44–63 polyclonal antibody) binds the same vesicle (arrow), as well as the RPE cytoplasm. (*J*) In merged images of different amyloid vesicles, punctate regions of both APP (blue, arrowheads) and Aβ immunoreactivity (green) are apparent. Areas of light blue fluorescence are indicative of APP and Aβ colocalization (arrows). (*K*) Double-label image showing the distributions of Aβ (red; Cy3) and APP (green; Cy2) in cultured human RPE cells. APP shows diffuse cytoplasmic staining, whereas punctate Aβ immunoreactivity is concentrated in the perinuclear region. (*L*) Anti-Aβ labeling of cultured human RPE cell cytoplasm is abrogated by preadsorption of anti-Aβ antibody (4G8) with A$\beta_{1\rightarrow42}$ peptide. (*M–O*) Double-label confocal immunofluorescence images showing the distributions of Aβ (green; Cy2) and iC3b, an activation-specific fragment of complement C3 (red; Cy3), in amyloid vesicles. The vesicular surface is punctated by discrete, as well as overlapping, areas of Aβ and/or iC3b immunoreactivity (*M*). A merged projection series (*N*) shows that most iC3b immunoreactivity is concentrated in the interior of the vesicles, whereas Aβ predominates in the outer shell. This is illustrated most dramatically in a single optical section (*O*) through the same vesicle shown in *N*. Note that discrete areas of colocalization (yellow) are also present on the outer shell (arrows in *M* and *N*). BM, Bruch's membrane; D, drusen.

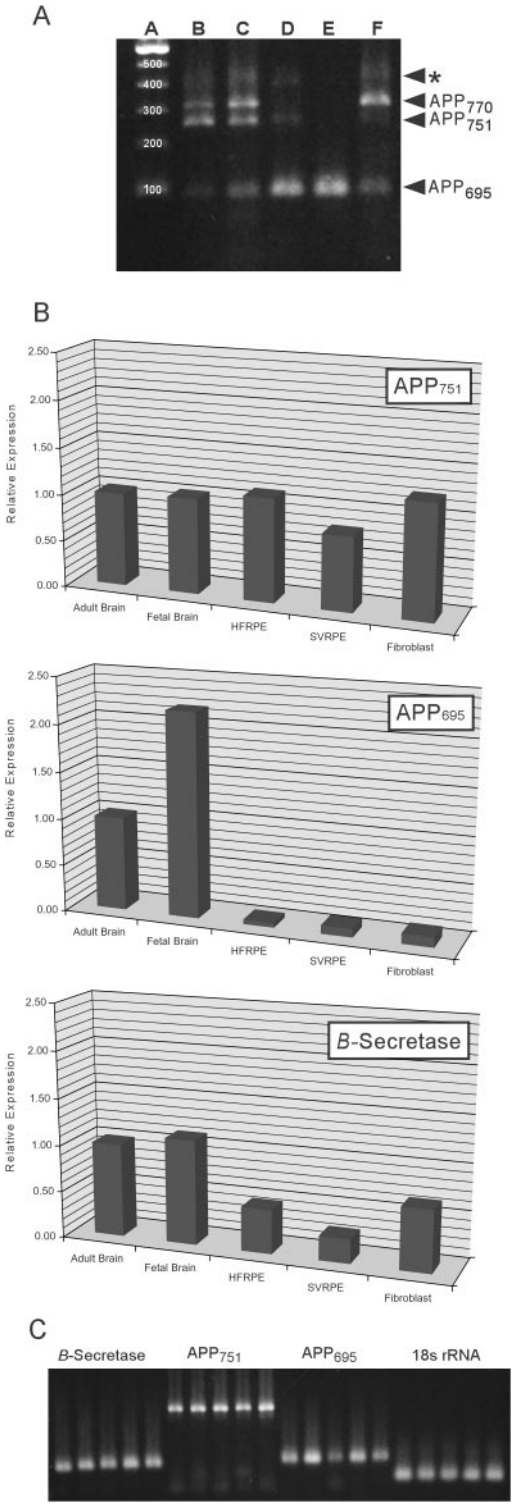

Fig. 3. PCR analyses of APP and β-secretase expression by human RPE cells relative to human brain and primary human fibroblasts. (*A*) Endpoint PCR analysis of APP isoform expression. Primary RPE cell cultures (lane B), as well as an SV40 transformed RPE cell line (lane C), express transcripts for the three major APP isoforms (APP_{770}, APP_{751}, and APP_{695}). A similar pattern of expression is observed in primary fibroblast cultures (lane F). The APP_{695} isoform predominates in both the adult (lane D) and fetal (lane E) brain, as has been reported (25). A fourth unidentified amplicon (asterisk) was detected in all samples examined. Lane A is a 100-bp size reference ladder. (*B*) Quantitative PCR analyses of the expression of APP_{751}, APP_{695}, and β-secretase. APP_{751} transcripts are expressed at similar levels in primary RPE cell cultures (HFRPE), SV40 transformed RPE cells (SVRPE), fibroblasts, and in both adult and fetal brain. In contrast, the expression level of APP_{695} in primary RPE cells is 20-fold lower than in adult brain, and more than 40-fold lower than in fetal brain. Similar expression levels are exhibited by SVRPE cells and normal human fibroblasts. The β-secretase expression level in primary RPE cells is approximately one-half of the level in the brain samples. In comparison to the primary RPE cells, SVRPE cells and fibroblasts have somewhat lower and higher β-secretase expression levels respectively. (see also Table 1). (*C*) Gel analysis of PCR products from the quantitative PCR analyses demonstrating the amplification of appropriately sized products for β-secretase (121 bp), APP_{751} (378 bp), APP_{695} (125 bp), and 18s rRNA (67 bp). (Lane 1, adult brain; Lane 2, fetal brain; lane 3, primary RPE; lane 4, SV40 RPE; lane 5, fibroblasts).

Table 1. Expression levels of APP_{751}, APP_{695}, and β-secretase

	APP_{751}	APP_{695}	β-Secretase
Adult brain	1.00	1.00	1.00
Fetal brain	1.02 ± 0.13	2.18 ± 0.32	1.12 ± 0.23
Primary RPE	1.11 ± 0.10	0.05 ± 0.01	0.47 ± 0.08
SV40 RPE	0.80 ± 0.08	0.09 ± 0.10	0.26 ± 0.07
Fibroblasts	1.23 ± 0.22	0.11 ± 0.02	0.66 ± 0.15

Normalized values (±SEM) relative to the adult brain sample arbitrarily set at 1.00.

gregates that consist of a central core and a peripheral "halo" (42). Recently, structures that are similar in size and morphology to those reported here, and that display Aβ immunoreactivity using the 6E10 anti-Aβ monoclonal antibody, have been identified in the brains of transgenic mice expressing human APP (43).

The evidence obtained in this study points strongly toward an RPE origin for amyloid vesicles. Significant APP immunoreactivity is present in the RPE cytoplasm, and Aβ immunoreactivity is often found in the cytoplasm of RPE cells that flank or overlie drusen. Secondly, anti-Aβ-labeled structures resembling amyloid vesicles can be identified intracellularly in the RPE cell cytoplasm. Third, cultured human RPE cells label with APP and Aβ antibodies, and contain transcripts for all three APP isoforms, as well as β-secretase. All of these findings are consistent with the conclusion that the RPE has the capacity to synthesize significant amounts of APP, and to generate Aβ through enzymatic processing. Thus, the available evidence suggests that the amyloid vesicles in drusen are derived from degenerate RPE cells that contain Aβ and, perhaps, other molecules highly resistant to proteolytic degradation.

It is now widely acknowledged that the formation of abnormal pathologic deposits in AD and other diseases is accompanied by chronic localized inflammation that can accentuate the effects of primary pathologic stimuli (1, 44, 45). The results presented here reinforce a growing body of evidence suggesting that AMD should now be added to this list (6–9). In a recent prospective population-based study, Klaver *et al.* (46) identified an increased risk of developing AD in individuals with advanced AMD. This association was attributed in part to smoking and atherosclerosis, significant risk factors for both AMD and AD, but could also be indicative of common pathogenic mechanisms in these diseases.

Although there is mounting and persuasive evidence of a primary pathogenic role for Aβ in AD, it is premature to suggest that Aβ plays a similar role in AMD. Drusen and amyloid plaques are regarded as the "hallmark lesions" of AMD and AD, respectively, but a causal role for drusen in AMD has not been established conclusively. Drusen, especially the nodular or so-called "hard" phenotype, are present in the eyes of many older individuals who do not show a clinically significant loss of visual acuity. Accordingly, some adhere to the view that drusen have no profound pathogenic role in AMD. Others link drusen, and the atrophic and neovascular changes characteristic of advanced

AMD, together as part of a pathologic continuum. An analogous divergence of opinion concerning the causative role of Aβ and amyloid plaque formation in AD has existed for some time.

The data presented in this study strongly implicate Aβ as a candidate activator of the complement cascade in the context of drusen formation. Additional investigations of a potential causal link between Aβ, drusen, and the development AMD are now warranted. In that regard, it will be important to determine the degree to which the similarities in molecular composition between AD and AMD lesions extend to shared pathogenic events that are manifested in the form of chronic local inflammation and Aβ-induced cytotoxicity.

We acknowledge the expert technical assistance of Tiffany Castillo, Adrienne Lightfoot, Kevin Talaga, and Sara Twogood. We are indebted to Paula Ousley and Rory Dunaway of the Oregon Lions Eye Bank for their invaluable assistance. The insights of Dr. Ratnesh Lal are also greatly appreciated. This work was supported by National Eye Institute Grants EY11527 (to L.V.J.) and EY11521 (to D.H.A.), and by generous benefactors of the Center for the Study of Macular Degeneration.

1. Akiyama, H., Barger, S., Barnum, S., Bradt, B., Bauer, J., Cole, G. M., Cooper, N. R., Eikelenboom, P., Emmerling, M., Fiebich, B. L., *et al.* (2000) *Neurobiol. Aging* **21,** 383–421.
2. Bradt, B. M., Kolb, W. P. & Cooper, N. R. (1998) *J. Exp. Med.* **188,** 431–438.
3. Webster, S., Lue, L. F., Brachova, L., Tenner, A. J., McGeer, P. L., Terai, K., Walker, D. G., Bradt, B., Cooper, N. R. & Rogers, J. (1997) *Neurobiol. Aging* **18,** 415–421.
4. Rogers, J., Cooper, N. R., Webster, S., Schultz, J., McGeer, P. L., Styren, S. D., Civin, W. H., Brachova, L., Bradt, B., Ward, P., *et al.* (1992) *Proc. Natl. Acad. Sci. USA* **89,** 10016–20.
5. McGeer, P. L., Akiyama, H., Itagaki, S. & McGeer, E. G. (1989) *Can. J. Neurol. Sci.* **16,** 516–527.
6. Johnson, L. V., Letiner, W. P., Staples, M. K. & Anderson, D. H. (2001) *Exp. Eye Res.* **73,** 887–896.
7. Johnson, L. V., Ozaki, S., Staples, M. K., Erickson, P. A. & Anderson, D. A. (2000) *Exp. Eye Res.* **70,** 441–449.
8. Hageman, G. S., Luthert, P. J., Chong, N. H. V., Johnson, L. V., Anderson, D. H. & Mullins, R. F. (2001) in *Progr. Ret. Eye Res.*, eds. Osborne, N. N. & Chader, G. J. (Elsevier Science, London), Vol. 20, pp. 705–732.
9. Anderson, D. H., Mullins, R. F., Hageman, G. S. & Johnson, L. V. (2002) *Am. J. Ophthalmol.* **134,** 411–431.
10. Sarks, S. H. (1982) *Aust. J. Ophthalmol.* **10,** 91–97.
11. Bressler, N. M., Silva, J. C., Bressler, S. B., Fine, S. L. & Green, W. R. (1994) *Retina* **14,** 130–142.
12. Mullins, R. F., Russell, S. R., Anderson, D. H. & Hageman, G. S. (2000) *FASEB J.* **14,** 835–846.
13. Lin, H. & Clegg, D. O. (1998) *Invest. Ophthalmol. Visual Sci.* **39,** 1703–1712.
14. Aronson, J. F. (1983) *In Vitro* **19,** 642–650.
15. Anderson, D. H., Johnson, L. V. & Hageman, G. S. (1995) *J. Comp. Neurol.* **360,** 1–16.
16. Hilbich, C., Monning, U., Grund, C., Masters, C. L. & Beyreuther, K. (1993) *J. Biol. Chem.* **268,** 26571–26577.
17. Kim, K. S., Miller, D. L., Sapienza, V. J., Chen, C. M. J., Bai, C., Grundke-Iqbal, I., Currie, J. R. & Wisniewski, H. M. (1988) *Neurosci. Res. Comm* **2,** 121–130.
18. Kim, K. S., Wen, G. Y., Bancher, C., Chen, C. M. J., Sapienza, V. J., Hong, H. & Wisniewski, H. M. (1990) *Neurosci. Res. Commun.* **7,** 113–122.
19. Golde, T. E., Estus, S., Usiak, M., Younkin, L. H. & Younkin, S. G. (1990) *Neuron* **4,** 253–267.
20. Bustin, S. A. (2000) *J. Mol. Endocrinol.* **25,** 169–193.
21. Beckman, M. & Iverfeldt, K. (1997) *Neurosci. Lett.* **221,** 73–76.
22. Ozaki, S., Johnson, L. V., Mullins, R. F., Hageman, G. S. & Anderson, D. H. (1999) *Biochem. Biophys. Res. Commun.* **258,** 524–529.
23. Simpson, D. A., Feeney, S., Boyle, C. & Stitt, A. W. (2000) *Mol. Vis.* **6,** 178–183.
24. Wilson, C. A., Doms, R. W. & Lee, V. M. (1999) *J. Neuropathol. Exp. Neurol.* **58,** 787–794.
25. Selkoe, D. J. (1994) *Annu. Rev. Neurosci.* **17,** 489–517.
26. Hageman, G. S., Mullins, R. F., Russell, S. R., Johnson, L. V. & Anderson, D. H. (1999) *FASEB J.* **13,** 477–484.
27. Anderson, D. H., Ozaki, S., Nealon, M., Neitz, J., Hageman, G. S. & Johnson, L. V. (2001) *Am. J Ophthalmol.* **131,** 767–781.
28. Curcio, C. A., Millican, C. L., Bailey, T. & Kruth, H. S. (2001) *Invest. Ophthalmol. Visual Sci.* **42,** 265–274.
29. Morgan, B. P. (1999) *Crit. Rev. Immunol.* **19,** 173–198.
30. Eikelenboom, P. & Stam, F. C. (1982) *Acta Neuropathol.* **57,** 239–242.
31. Hamazaki, H. (1995) *Biochem. Biophys. Res. Commun.* **211,** 349–353.
32. Matsubara, E., Frangione, B. & Ghiso, J. (1995) *J. Biol. Chem.* **270,** 7563–7567.
33. Evans, K. C., Berger, E. P., Cho, C. G., Weisgraber, K. H. & Lansbury, P. T., Jr. (1995) *Proc. Natl. Acad. Sci. USA* **92,**763–767.
34. Eriksson, S., Janciauskiene, S. & Lannfelt, L. (1995) *Proc. Natl. Acad. Sci. USA* **92,** 2313–2317.
35. Schwarzman, A. L., Gregori, L., Vitek, M. P., Lyubski, S., Strittmatter, W. J., Enghilde, J. J., Bhasin, R., Silverman, J., Weisgraber, K. H., Coyle, P. K., *et al.* (1994) *Proc. Natl. Acad. Sci. USA* **91,** 8368–8372.
36. Loeffler, K., Edward, D. & Tso, M. (1995) *Invest. Ophthalmol. Visual Sci.* **36,** 24–31.
37. Burns, R. P. & Feeney-Burns, L. (1980) *Trans. Am. Ophthalmol. Soc.* **78,** 206–225.
38. Ishibashi, T., Patterson, R., Ohnishi, Y., Inomata, H. & Ryan, S. J. (1986) *Am. J. Ophthalmol.* **101,** 342–353.
39. Curcio, C. A. & Millican, C. L. (1999) *Arch. Ophthalmol.* **117,** 329–339.
40. Russell, S. R., Mullins, R. F., Schneider, B. L. & Hageman, G. S. (2000) *Am. J. Ophthalmol.* **129,** 205–214.
41. Ulshafer, R. J., Allen, C. B., Nicolaissen, B., Jr., & Rubin, M. L. (1987) *Invest. Ophthalmol. Visual Sci.* **28,** 683–689.
42. Westlind-Danielsson, A. & Arnerup, G. (2001) *Biochemistry* **40,** 14736–14743.
43. Terai, K., Iwai, A., Kawabata, S., Tasaki, Y., Watanabe, T., Miyata, K. & Yamaguchi, T. (2001) *Neuroscience* **104,** 299–310.
44. Nangaku, M. (1998) *Kidney Int.* **54,** 1419–1428.
45. Torzewski, J., Bowyer, D. E., Waltenberger, J. & Fitzsimmons, C. (1997) *Atherosclerosis* **132,** 131–138.
46. Klaver, C. C., Ott, A., Hofman, A., Assink, J. J., Breteler, M. M. & de Jong, P. T. (1999) *Am. J. Epidemiol.* **150,** 963–968.